Nanoscale

PAPER

Cite this: *Nanoscale*, 2016, **8**, 1470

Noncovalent functionalization of solid-state nanopores *via* self-assembly of amphipols†

Gonzalo Pérez-Mitta,[a] Loïc Burr,[b,c] Jimena S. Tuninetti,[a] Christina Trautmann,[b,c] María Eugenia Toimil-Molares[b] and Omar Azzaroni*[a,d]

Received 19th November 2015,
Accepted 20th November 2015

DOI: 10.1039/c5nr08190d

www.rsc.org/nanoscale

In recent years there has been increasing interest in the development of new methods for conferring functional features to nanopore-based fluidic devices. In this work, we describe for the first time the non-covalent integration of amphoteric–amphipathic polymers, also known as "amphipols", into single conical nanopores in order to obtain signal-responsive chemical nanodevices. Highly-tapered conical nanopores were fabricated by single-sided chemical etching of polycarbonate foils. After etching, the surface of the conical nanopores was chemically modified, by first metallizing the surface *via* gold sputtering and then by amphiphilic self-assembly of the amphipol. The net charge of adsorbed amphipols was regulated *via* pH changes under the environmental conditions. The pH-dependent chemical equilibrium of the weak acidic and basic monomers facilitates the regulation of the ionic transport through the nanopore by adjusting the pH of the electrolyte solution. Our results demonstrate that functional amphipathic polymers are powerful building blocks for the surface modification of nanopores and might ultimately pave the way to a new means of integrating functional and/or responsive units within nanofluidic structures.

Introduction

Bioinspired nanofluidic devices for on-demand control of ion transport on the nanoscale are attracting scientific and technological interest owing to the outstanding properties and functionalities[1] that can be achieved as well as the wide range of potential applications they offer in multiple fields, including molecular sieves,[2] nanofluidics,[3] energy conversion,[4] and biosensors.[5] Recent progress in this field has enabled the reproducible fabrication of synthetic nanopores displaying properties that mimic their biological counterparts. Compared with lipid membranes, which are difficult to manipulate, solid state single nanopores constitute a more suitable paradigm owing to their robust mechanical and chemical properties.[6] Single conical nanopores are able to rectify the ion transport through them, which is in close resemblance to voltage-gated biological ion channels.[7] As a result, the generation of "fully synthetic" architectures with functionalities comparable to biological entities has stimulated scientists from diverse disciplines, including chemistry, physics and engineering.[8]

The versatility of synthetic nanopores is already visible in multiple applications and is based on the multifunctional physical and chemical properties. Based on numerous studies, great advances in molecular design, in understanding the relationships between pore geometry and current rectification, and in efficient processing strategies have been achieved. Nanoscale control over the surface properties of the pore walls is an important issue because chemical functionalization can modulate nanopores' unique rectifying characteristics arising from the synergy of the entropic driving force caused by the channel asymmetry and the electrostatic effects due to the charges fixed on the pore wall.[9–11] The development of new means to manipulate both the geometry and the surface charge of conical nanopores is extremely important for future applications.

The development of functionalized conical nanopores with adjustable rectification properties resulting from external modulation of surface charges has attracted considerable attention. The efficiency with which many pore-forming proteins in biological membranes control the ionic transport using pH as a chemical trigger has been a source of inspiration for chemists to mimic such processes using functionalized nanopores.[12] In the case of biological pores their amphoteric nature originating from ionizable amino acid residues and protonable amine groups is responsible for dictating the ion

[a]*Instituto de Investigaciones Fisicoquímicas Teóricas y Aplicadas (INIFTA), Departamento de Química, Facultad de Ciencias Exactas, Universidad Nacional de La Plata, CONICET, CC 16 Suc. 4 (1900) La Plata, Argentina. E-mail: azzaroni@inifta.unlp.edu.ar*

[b]*GSI Helmholtzzentrum für Schwerionenforschung, Planckstraße 1, 64291 Darmstadt, Germany*

[c]*Materialwissenschaft, Technische Universität Darmstadt, Alarich-Weiss-Straße 2, 64287 Darmstadt, Germany*

[d]*Consejo Nacional de Investigaciones Científicas y Técnicas (CONICET), Argentina*

†Electronic supplementary information (ESI) available. See DOI: 10.1039/c5nr08190d

selectivity.[13] One illustrative example is the cornea where the ion permselectivity is controlled by the degree of protonation of ionizable sites within the tissue.[14]

A pioneering study by Martin and co-workers described the pH-switchable permselectivity of cylindrical cysteine-modified gold-coated nanotubes, demonstrating the capabilities of zwitterionic moieties to tailor the surface charge of nanopore environments.[15] These concepts were further extended to the manipulation of the rectification properties of conical nanopores using monolayer assemblies and polymer brushes grafted on the pore walls.[16]

To the best of our knowledge, tailoring the surface charge in single conical nanopores has been performed almost exclusively using covalent chemistries featuring varied complexity. For many years, chemical functionalization of track-etched pores in polymers like polyethylene terephthalate (PET), polycarbonate (PC) and polyimide (PI) has been focused exclusively on the derivatization of the residual surface carboxyl group with alkyl bromide in the presence of KF as a catalyst,[17] methylation with diazomethane,[18] or amidation *via* activation of surface carboxyl groups with carbodiimide and subsequent reaction with amine-terminated linkers bearing the targeted functionality.[19] However, many of these preparative protocols involve the use of organic solvents in consecutive reaction steps, which might compromise the structural stability of the pore. This factor is particularly predominant in the case of nanoscale pores where small variations in pore dimension can lead to drastic changes in rectification properties. Within this framework, it is particularly desirable to develop methods for non-covalent functionalization of nanopores without requiring demanding protocols.

For this purpose, amphiphilic self-assembly[20] offers a rapid and suitable method to functionalize solid-state nanopores owing to the simplicity and tractability of the hydrophobic interactions that ultimately allow functional films to be designed and built up through very simple steps.[21] For instance, extensive work of Armes and co-workers demonstrated that direct adsorption of amphiphilic copolymers from solution can lead to the formation of a broad variety of stimulus-responsive surfaces.[21,22]

In spite of the potential practical advantages, the use of amphiphilic self-assembly as a noncovalent strategy to functionalize asymmetric solid-state nanopores and to manipulate their rectification properties is presently unexplored. Taking into account existing insights from studies on amphiphilic polymer solutions and being aware of the potential benefits derived from the facile non-covalent integration of responsive units into solid-state nanopores, the goal of this work is to explore this new conceptual paradigm by creating an amphoteric pH-tunable nanofluidic diode. We demonstrate that the hydrophobic assembly of amphoteric–amphipathic polymers, known as "amphipols",[23] provides a promising, robust and noncovalent strategy to fine-tune the rectifying characteristics of nanopores with the option to manipulate the mass or ion transport through them by simply varying the environmental pH.

Results and discussion

Several methods have been developed to obtain a longitudinal asymmetry in the charge distribution of polymer nanopores. Among these, anisotropic chemical etching that produces conical geometries has been the most used one, as a consequence of its versatility.[1,2] Herein, the use of 30 μm long tapered conical PC nanopores as nanofluidic diodes is introduced. In order to fully characterize the geometry of the nanopores, Au has been electrodeposited using the replica technique using multitrack-etched foils as templates (Fig. 1(a) and (b)). The nanocones adopt the shape and size of the channels and exhibit base diameters of ~4000 nm and tip diameters with values of ~60 nm. Here, the well-defined conical shape of the nanopores can be clearly seen. The diameter of the large opening of the nanopores was also observed by SEM imaging (Fig. 1(c) and Fig. 1 in the ESI†), finding values that resemble those obtained by the replica technique.

After the etching, the nanopores were metalized with sputtering of Au over the tip side. In order to characterize the ionic conductivity of the nanopores, *I–V* measurements were made before and after (Fig. 2(a)) metallization with gold sputtering. As can be seen in Fig. 2(a), there is an increase in the rectification factor from −2.5 to −9 as well as a decrease in the ionic conductivity from 345 nS to 98 nS after metallization. The effect of improving the rectification of nanopores with one-sided metal sputtering has been reported previously by Hou *et al.*[24] The layer of gold is expected to have a thickness in the direction normal to the surface of about 80 nm as calculated from the calibration of the sputtering machine.

Regarding the characteristics of current–voltage curves, it was observed that at high negative potentials, the current becomes non-linear with the voltage with a saturation tendency (Fig. 2(a)). Even though there are previous reports of this effect on solid-state nanopores in the literature, as far as we know there is still no satisfactory model to explain it.[25] However, a possible explication of this effect could be found in the typical behavior of cation-exchange membranes, in which the permselectivity of the membranes generates a concentration polarization throughout the membrane pores that produces a limiting current region at high voltages.[26,27] Further efforts, both experimental and theoretical, are needed to fully elucidate this issue.

The proposed procedure to functionalize the nanopore through noncovalent interactions is depicted in Scheme 1. In this approach, the amphoteric–amphiphilic polymer (amphipol) adsorbs noncovalently onto the exposed surfaces from aqueous solutions *via* hydrophobic interactions. The noncovalently attached layer of amphipols contains carboxylic acid groups and tertiary amines that can be used as pH-tunable moieties, thus forming a responsive coating.

In order to test the viability of this strategy we first demonstrated and optimized the proposed method using planar gold-coated surfaces as model substrates. The irreversible noncovalent functionalization of gold substrates was confirmed by using surface plasmon resonance spectroscopy (SPR). Analyz-

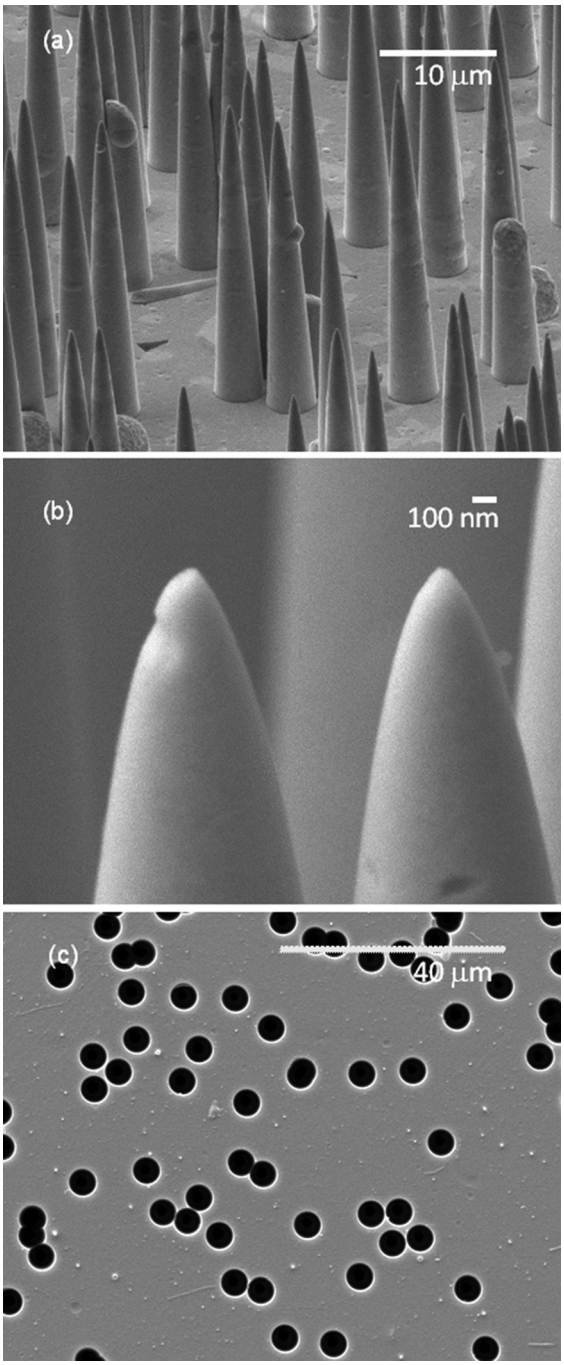

Fig. 1 SEM images of gold nanocones fabricated by the replica technique using a multitrack-etched polycarbonate membrane, the scale bars represent (a) 10 μm and (b) 100 nm. (c) SEM image of a multitrack etched foil showing the base of the nanopores after etching, showing a base of ~4000 nm.

ing the SPR sensorgram (Fig. 2b), in the case of an aqueous amphipol solution (1 mg ml^{-1}) flowing through the SPR liquid cell, a sharp increase in the SPR signal is observed that does not decrease even after extensive rinsing in deionized water. This fact is indicative of the presence of an amphipol layer irreversibly deposited onto the gold-coated SPR chip with a surface coverage of 85 ng cm^{-2} and a thickness of ~1 nm. This value implies that the amphipol coating of the surface corresponds to a single layer. The amphipol-modified surface was further characterized using infrared spectroscopy (IR) and contact angle (CA) measurements to corroborate the presence of their functional groups (Fig. 2(c) and (d)). IR measurements confirmed the success of the modification strategy by showing the appearance of characteristic bands corresponding to the functional groups present in the amphipol polymer (Fig. 2(c)). On the other hand considering that in most cases alkyl-terminated surfaces exhibit a CA of ~90°,[28] our wetting measurements close to 60° suggest that the aliphatic tails of the amphipathic architecture are not located in the outermost region of the polymer layer but they will probably be located at the surface–polymer interface. In a similar context, we can infer from the wetting measurements that the ionizable groups of the amphipols are oriented towards the aqueous solution.[28]

Having demonstrated the ability to functionalize gold surfaces with amphipols, we next extended this concept to the noncovalent functionalization of polymer nanopores. As mentioned above, PC membranes containing a single nanopore were only coated on the tip side with a gold layer to homologate the working substrate in accordance with SPR results.

Then, the previously metallized single nanopore membranes were modified by simple immersion in an aqueous solution of amphipol for 2 hours. Afterwards, the membranes were thoroughly rinsed with Milli-Q water and mounted on the conductivity cell. Fig. 3 shows the *I–V* curves of a single conical nanopore modified with amphipol using 0.1 M KCl (at different pHs) as the electrolyte solution in both half-cells. Considering the amphoteric nature of the adsorbed amphipathic polymer (Scheme 1) we can infer that at strongly acidic pHs the tertiary amine decorating the pore wall will bear positively charged groups corresponding to $-N(CH)_2H^+$. As is well-known, the presence of rectification requires surface charges with an asymmetric longitudinal distribution that is generally achieved by an asymmetry in the geometry of the nanopore, for example, with a conical shape. In our case we observed that at pH 2 the *I–V* curve displayed a well-defined rectification behavior which would imply the permselective transport of anionic chloride species through the positively charged nanopore (Fig. 3). The maximum rectification factor (f_{rec}), defined as the ratio between currents measured at given voltages (1 V in this case) but at opposite polarities, was ~−12 at high pHs and ~8 at low pHs. These results are higher than those previously reported in the literature using polymer nanopores decorated with monolayer assemblies, $f_{rec} \sim 4$, and are comparable to reported values using nanopores decorated with polymer brushes.[29,30]

Fig. 3 shows the effect of pH on the *I–V* curves of an amphoteric nanopore noncovalently functionalized *via* amphiphilic self-assembly of amphipols. At low pH values, the tertiary amines are positively charged due to protonation, while the carboxylic groups (–COOH) are neutral under such acidic conditions. The positive charges decorating the pore walls render the nanopore selective to anions and consequently the nano-

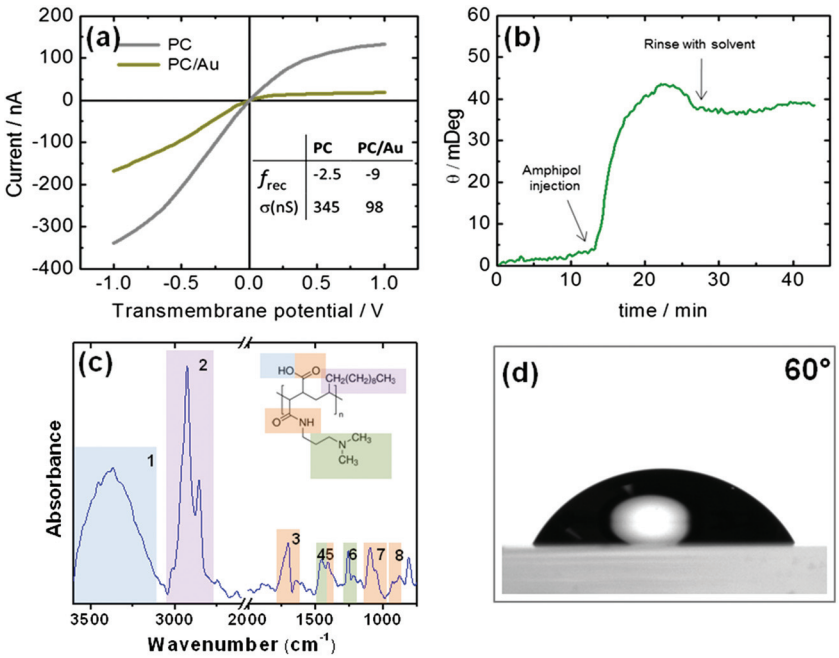

Fig. 2 (a) Current–voltage curve of a conically-etched nanopore before (PC, grey curve) and after (PC/Au, dark yellow curve) sputtering of gold over the tip side. The inset shows the rectification factor f_{rec} and the ionic conductivity σ (nS) before and after gold sputtering. (b) Changes in the angle of the reflection minimum as a function of time during the adsorption of amphipol (1 mg ml^{-1}) on a bare gold surface. The signal indicates that the amphipol remains immobilized on the substrate after rinsing with the aqueous solvent. (c) ATR-FTIR spectrum of a gold surface modified with an amphipol monolayer. IR signals correspond to: (1) 3100–3600 cm^{-1} amine and amide N–H stretching and O–H stretching (acid), (2) 2800–3100 cm^{-1} aliphatic C–H stretching, (3) 1705–1780 cm^{-1} C=O stretching (acid), 1653 cm^{-1} amide C=O stretching, (4) 1460 cm^{-1} antisymmetric bending C–H in *N*,*N*-dimethyl amine, (5) 1410 cm^{-1} C–O–H acid in-plane bending, (6) 1262 cm^{-1} amide C–N stretching, (7) 1100 cm^{-1} acid C–O stretching, and (8) 900–935 cm^{-1} O–H out-of-plane bending (acid). (d) Contact angle measurement of a gold surface after the modification with an amphipol layer.

fluidic device shows the typical rectification properties of conical pores with positive fixed charges. In functional terms this translates into a high conducting ("ON") state for $V > 0$ and a low conducting ("OFF") state for $V < 0$. On the other hand, at high pH values, the tertiary amine groups ($-N(CH)_2$) are deprotonated (in neutral form), but carboxylic groups ($-COO^-$) are ionized. As a result, the pore bears negative charges on the walls and the nanofluidic diode is now selective to cations. Contrary to that observed at low pHs, the "ON" and "OFF" states under alkaline conditions appear at $V < 0$ and $V > 0$, respectively. The transition between both rectification regimes occurs at pH = 5, which is the apparent isoelectric point, IP^{app}, of the amphipol and is characterized by a non-rectifying state.

Fine-tuning of surface charges and rectification properties was demonstrated through *I*–*V* measurements carried out under different pH conditions. As described in Scheme 1, the amphoteric nature of the monomer units involves a variety of charged states that are thermodynamically controlled by the pH value. Fig. 4 shows the effect of gradual changes in pH on the *I*–*V* curves of the functionalized nanopore. Upon increasing the pH from 2.2 to 3 the population of "zwitterionic" monomer units grows at the expense of the $-N(CH)_2H^+$ species resulting in a "less positive" net surface charge. The *I*–*V* curve indicates that at pH ~ 3 a well-defined rectification behavior is still observed, but the rectified current is decreased. Note that the presence of positive charges in the pore walls promotes the exclusion of cations from the nanofluidic device and consequently the "OFF" state of cation-driven rectified ionic currents may be observed at each pH value below IP^{app}, even though the "ON" state of anion-driven rectified ionic currents can be easily tuned by slight pH variations (Fig. 5). This fact clearly indicates that the surface-attached amphipol enables the tuning of the rectified current under the same permselective conditions.

Increasing the pH to 4.5 resulted in a significant loss of both the conductivity and the rectification behavior of the pore. At the apparent isoelectric point of the amphipol the net charges are zero and the nanopore is nonselective to ions (anions and cations), leading to the loss of rectification and to a decrease in the ionic conductivity, namely a gating effect. However, at pH 7.4 the presence of negative net charges gives rise to the ionic current and to the rectifying characteristics depicted in Fig. 4. Further increase in pH above the apparent isoelectric point (IP^{app}) implies a further displacement of the zwitterionic equilibrium toward the formation of negatively charged species (COO^-), thus reversing the permselectivity and rectification characteristics observed at acidic pHs.

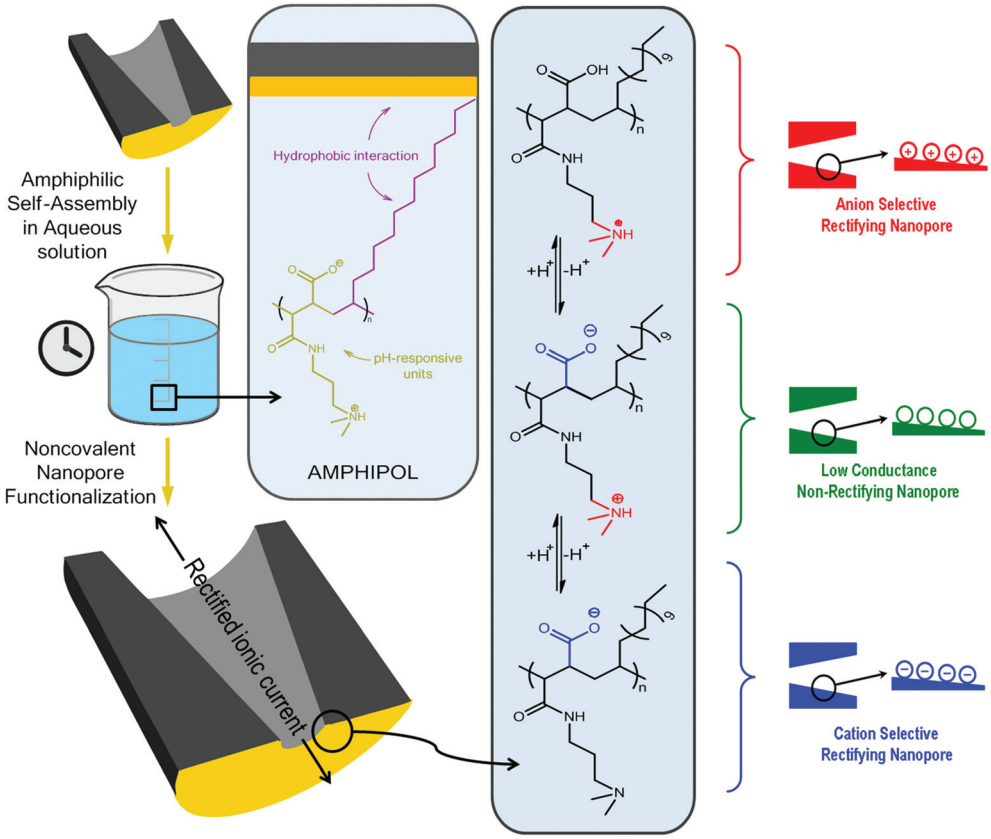

Scheme 1 Schematic cartoon of the noncovalent functionalization of a conical nanopore with amphipols. The chemical structure of the amphiphilic–amphoteric polymer and the equilibrium associated with the pH-dependent behavior of the ionizable-protonable monomer units are indicated. The cartoon on the right side shows the net charge of the tip surface at low pH (red, positive net charge), at the isoelectric point (green, no net charge) and at high pH (blue, negative net charge).

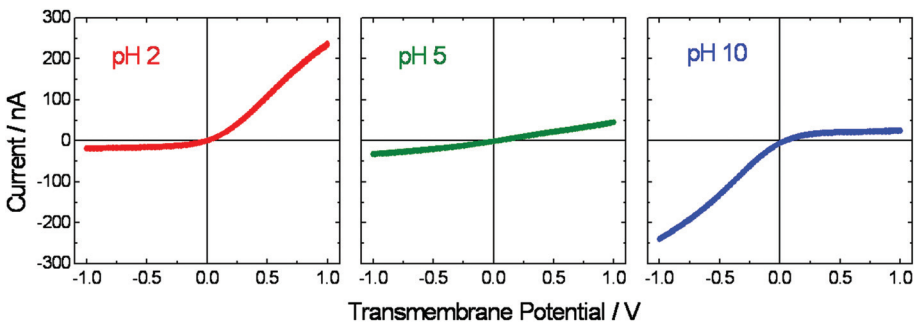

Fig. 3 Current–voltage curves of a single amphipol-modified conical nanopore at different proton concentrations: (left) pH = 2, (center) pH = 5, and (right) pH = 10. The three curves were measured with the same nanopore. The nanopore used during these experiments displayed the following dimensional characteristics: base diameter ~4000 nm and tip diameter ~60 nm.

In opposition to the trend observed under acidic conditions, the presence of negative charges at high pH values triggers the exclusion of anions from the pore and the "OFF" state of anion-driven ionic currents is observed at pH > IP^{app} whereas the cation-driven "ON" state can be easily modulated and amplified by increasing the pH (Fig. 5). Taken together, these experiments show that displacement of the protonation equilibrium of the noncovalently anchored amphipols enables the modulation of the ionic selectivity and rectification characteristics by changing the proton concentration in a broad pH range.

Fabrication of amphoteric nanofluidic devices through noncovalent strategies poses interesting challenges in the framework of device stability. As is well known, pH alteration may cause structural reorganization of the amphoteric/amphipathic layer with concomitant effects on the functional properties

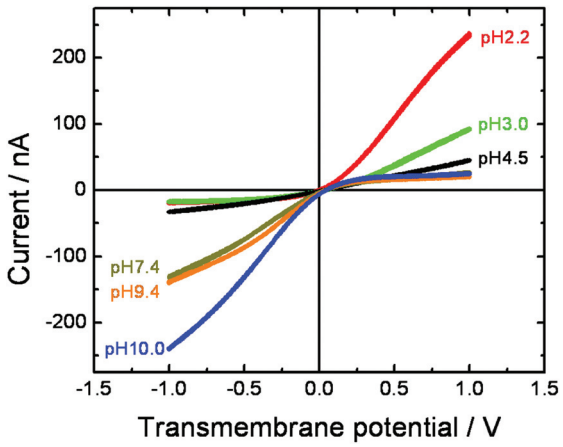

Fig. 4 *I–V* curves of a single conical nanopore modified with amphipols measured at different pH values (using 0.1 M KCl as the electrolyte). Nanopores used during these experiments displayed the following dimensional characteristics: base diameter ~4000 nm and tip diameter ~60 nm.

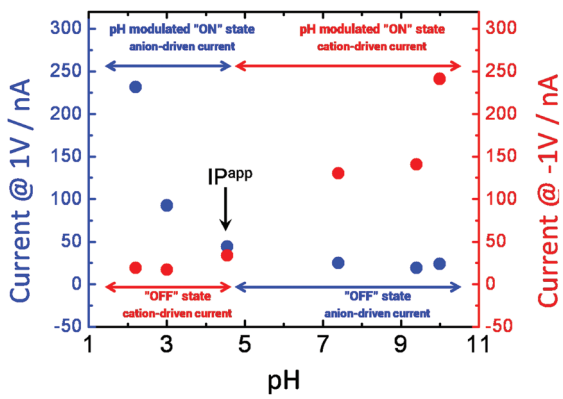

Fig. 5 Changes in rectified currents upon variation of the environmental pH. The red and blue data refer to the rectified currents measured at –1 and 1 V, respectively. In the plot are also indicated the regions corresponding to the "on" and "off" states of the anion- and cation-driven currents flowing through the nanofluidic diode.

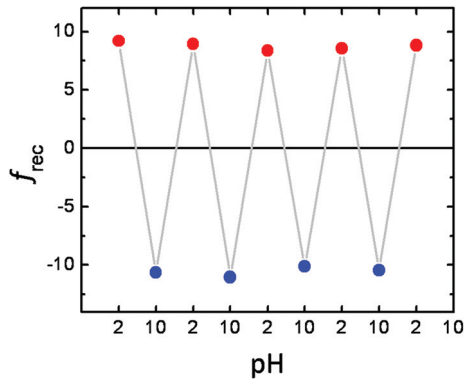

Fig. 6 Reversible variation of the rectified ionic current passing through an amphipol-modified nanofluidic diode upon alternating the environmental pH between 2 (red circles, "on" state: anion-driven current, "off" state: cation-driven current) and 10 (blue circles, "on" state: cation-driven current, "off" state: anion-driven current). Nanopores used during these experiments displayed the following dimensional characteristics: base diameter ~4000 nm and tip diameter ~60 nm.

and reversibility of the amphoteric fluidic diode. Hence, it is very important to demonstrate its reversibility under opposite pH conditions. With this in mind, we repeated the measurements of *I–V* curves using the same electrolyte solution at pH 2 and 10. The recordings were performed by manually changing the solutions in the conductivity cell used for the ionic current measurements. Fig. 6 presents the reversible variation of the transmembrane ionic current measured at ±1 V in the presence of consecutive pH changes between 2 and 10. These measurements confirm the excellent reversibility of the amphoteric nanofluidic device and provide conclusive evidence of the stability of the noncovalently attached amphipol layer. However, the system will lose its functionality after several days of storing it in water or in air, being possible to regain it by another immersion in the amphipol solution (the solution can be reused for this purpose). This fact is not necessarily a drawback as it permits the recycling of the nanopore for further experiments.

Furthermore, the complete experiment was repeated three times with different pores to prove the repeatability of the procedure, the results were conclusive in showing that the system can be fully replicated (see the ESI†).

For the purpose of gaining a complete understanding of the behaviour of the amphipol-modified nanofluidic diode we have explored the effect of the ionic strength on the current rectification efficiency of the system. In order to evaluate the effect of the electrolyte concentration, several *I–V* curves at different pH values were recorded using three different concentrations of KCl: 0.01 M, 0.1 M and 1 M. Fig. 7 shows the behaviour of the rectification factor with the pH at different KCl concentrations. It was found that there is no major difference between the curves at 0.01 M and 0.1 M in terms of the

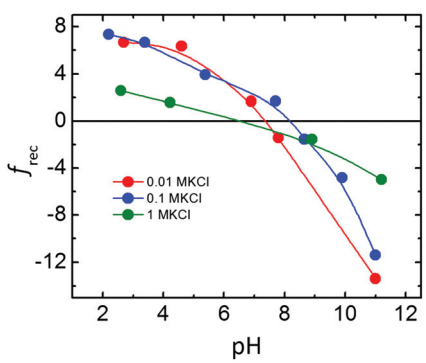

Fig. 7 Rectification factor *versus* pH for different KCl concentrations: 0.01 M (red curve), 0.1 M (blue curve) and 1 M (green curve). Nanopores used during these experiments displayed the following dimensional characteristics: base diameter ~4000 nm and tip diameter ~60 nm.

rectification efficiency as can be seen by comparing red and blue curves. However, there is a higher difference between the curves at 0.01 M and 0.1 M and the curve at 1 M in which the rectification efficiency is minor in the whole pH range. This effect could be understood by taking into account that a higher electrolyte concentration decreases the Debye length, thus increasing the screening of the surface charges. As a consequence, the permselectivity of the system to either cations or anions is reduced.

Another interesting difference in behaviour at different electrolyte concentrations is in the magnitude of the ionic current achieved. There is a 4-fold increment between the currents at 0.01 M and the currents at 0.1 M whilst there is a 6-fold increase between the measurements at 0.1 M and 1 M (Fig. 2 in the ESI†). This implies that by using different concentrations of electrolytes and different pH values, a complete tuning of the transport properties of the system can be achieved both in the rectification and the magnitude of the ionic current.

Conclusions

We have demonstrated the preparation of functional nanofluidic diodes by noncovalent amphipathic functionalization. Functional amphipathic polymers, also known as "amphipols", are powerful building blocks for spontaneous, one-pot surface modification of solid-state nanopores. The one-step approach employs a simple immersion in dilute aqueous solutions containing the amphipathic polymer with predefined amphoteric functions, resulting in amphiphilic self-assembly decoration of the pore surface with protonable/ionizable groups. The pH dependent chemical equilibrium of their monomer units allows fine-tuning of the ionic selectivity and rectified ionic transport. By presetting the environmental pH, noncovalent chemistries can provide a simple and robust means to endow nanofluidic diodes with unique features. This concept gains high relevance taking into consideration that very recently ligand-modified amphipols have been used to modify planar surfaces for biorecognition purposes. Hence, amphipols not only offer the possibility of tailoring the surface charge, but also the integration of recognition sites. The particular features of the amphipol assembly with respect to flexibility, speed, affordability, and functional versatility in combination with tailored transport properties of conical nanopores can open the door to novel signal-responsive chemical nanodevices.

Experimental section

Materials

Synthetic nanopores were fabricated in polycarbonate foils (Makrofol N, Bayer Leverkusen) (thickness = 30 μm). Poly(maleic anhydride-*alt*-1-tetradecene) and 3-(dimethylamino)-1-propylamine derivative (amphipol) were purchased from Sigma-Aldrich and used as received.

Conical nanopore fabrication

Polycarbonate foils were irradiated at the UNILAC (Universal Linear Accelerator) of GSI, Darmstadt with 2.2 GeV Au ions. The fluence was either 10^7 ions per cm^2 or a single ion per sample. Each ion creates a track which can be converted into an open channel by chemical etching. In order to obtain tapered conical nanopores, the irradiated foils were etched asymmetrically in a 2-compartment cell using a mixture of 40% of 6 M NaOH and 60% methanol as the etchant on one side of the membrane and distilled deionized water on the other. A voltage difference of 1 V was applied during etching and the temperature was controlled and set to 30 °C.[31] After the etching, *I–V* measurements were made to observe the ionic conductivity of each nanopore. Afterwards a gold layer was sputtered over the tip side of the membranes. The parameters were set so as to obtain a rate of deposition of 40 nm min^{-1}. The thickness of the layer normal to the surface was calculated to be ~80 nm under the experimental conditions.

Fabrication of gold nanocones

After sputter-coating one surface of the track-etched membrane, the pores of the multitrack-etched membrane were filled by electrodeposition of gold at a constant potential of −0.375 V (*vs.* Ag/AgCl reference) at 60 °C from a commercial Au sulphite bath (AuSF, 15 g L^{-1}, Metakem GmbH).[32,33] The membrane was then dissolved in dichloromethane and the resulting nanocones were imaged by scanning electron microscopy (JEOL JSM7401-F, 10 kV). An etching time of 15 min results in cone bases of about 2.5 μm while 30 minute etching leads to diameters of about 4 μm. In both cases, the tip size varied between 50 and 100 nm.

SPR measurements

A SPR Navi 210 equipment from Bionavis was used to measure the adsorption of the amphipols on the gold substrate. The flow rate during the experiment was adjusted to 10 μl min^{-1} and a concentration of 1 mg ml^{-1} of amphipol was used. WinSpall software was used to calculate the surface concentration and the thickness of the adsorbed layer.

FTIR spectroscopy

Fourier transform infrared spectroscopy in the attenuated total reflection mode was performed using a Varian 600 FTIR spectrometer equipped with a ZnSe ATR crystal with a resolution of 1 cm^{-1}. Background-subtracted spectra were corrected for ATR acquisition by assuming a refractive index of 1.45 for all of the samples.

Contact angle measurements

Contact angles were measured using a Ramé-Hart contact angle system (Model 290) at 25 °C. In each measurement, a 1 μL droplet of water was dispensed onto the modified surface. The average contact value was obtained at seven different positions of the same membrane.

I–V measurements

I–V curves were measured using a Gamry Reference 600 from Gamry Instruments with a scan rate of 100 mV s^{-1}. A 0.1 M KCl solution was used. The ground electrode, *i.e.* the counter-electrode, was placed always towards the tip of the nanopores to ensure a facile interpretation of the results. The pH was adjusted by adding dropwise either 0.5 M NaOH or 0.5 M HCl. The conductivity of the channel was calculated as the slope of the *I–V* curves in the range from −0.1 V to 0.1 V in which the curves behave linearly. The rectification factors (f_{rec}) were calculated as the quotient between the absolute values of the currents at either ±1 V or ±0.5 V. The value was multiplied by −1 when the higher currents were negative to assign a negative f_{rec} value to a negative surface charge.

Acknowledgements

The authors acknowledge financial support from ANPCyT (PICT 2010-2554 and PICT-2013-0905), Fundación Petruzza, the Austrian Institute of Technology GmbH (AIT–CONICET Partner Lab: "Exploratory Research for Advanced Technologies in Supramolecular Materials Science" – Exp. 4947/11, Res. No. 3911, 28-12-2011) and the Deutsche Forschungsgemeinschaft (DFG-FOR 1583). G. P.-M. and J. S. T acknowledge CONICET for a doctoral and a postdoctoral fellowship, respectively. O. A. is a CONICET fellow.

References

1 (*a*) X. Hou, W. Guo and L. Jiang, *Chem. Soc. Rev.*, 2011, **40**, 2385; (*b*) Y. Tian, L. Wen, X. Hou, G. Hou and L. Jiang, *ChemPhysChem*, 2012, **13**, 2455; (*c*) Z. S. Siwy, *Adv. Funct. Mater.*, 2006, **16**, 735–746; (*d*) Y. He, D. Gillespie, I. Vlassiouk, R. S. Eisenberg and Z. S. Siwy, *J. Am. Chem. Soc.*, 2009, **131**, 5194–5202; (*e*) Z. Siwy and A. Fulinski, *Am. J. Phys.*, 2004, **75**, 567–574; (*f*) Z. Siwy, P. Apel, D. Dobrev, R. Neumann, R. Spohr, C. Trautmann and K. Voss, *Nucl. Instrum. Methods Phys. Res., Sect. B*, 2003, **208**, 143–148.

2 C. R. Martin, M. Nishizawa, K. Jirage, M. Kang and S. B. Lee, *Adv. Mater.*, 2001, **13**, 1351.

3 J. C. T. Eijkel and A. van den Berg, *Chem. Soc. Rev.*, 2010, **39**, 957.

4 L. Wen, X. Hou, Y. Tian, F. Q. Nie, Y. Song, J. Zhai and L. Jiang, *Adv. Mater.*, 2010, **22**, 1021.

5 (*a*) W. Guo, Y. Tian and L. Jiang, *Acc. Chem. Res.*, 2013, **46**, 2834; (*b*) Z. Siwy, L. Trofin, P. Kohli, L. A. Baker, C. Trautmann and C. R. Martin, *J. Am. Chem. Soc.*, 2005, **127**, 5000–5001.

6 C. Dekker, *Nat. Nanotechnol.*, 2007, **2**, 209.

7 Z. Siwy, P. Apel, D. Baur, D. D. Dobrev, Y. E. Korchev, R. Neumann, R. Spohr, C. Trautmann and K.-O. Voss, *Surf. Sci.*, 2003, **532–535**, 1061–1066.

8 (*a*) B. M. Venkatesan and R. Bashir, in *Nanopores: Sensing and Fundamental Biological Interactions*, ed. S. M. Iqbal and R. Bashir, Spinger Verlag, New York, 2011, pp. 1–33; (*b*) T. Albrecht and J. B. Edel, in *Engineered Nanopores for Bioanalytical Applications*, ed. J. B. Edel and T. Albrecht, Elsevier, Waltham, 2013, pp. ix–xi.

9 S. Howorka and Z. Siwy, *Chem. Soc. Rev.*, 2009, **38**, 2360.

10 Z. Siwy, E. Heins, C. C. Harrell, P. Kohli and C. R. Martin, *J. Am. Chem. Soc.*, 2004, **126**, 10850.

11 I. D. Kosińska, I. Goychuk, M. Kostur, G. Schmid and P. Hänggi, *Phys. Rev. E: Stat., Nonlinear, Soft Matter Phys.*, 2008, **77**, 1.

12 F. Xia, W. Guo, Y. Mao, X. Hou, J. Xue, H. Xia, L. Wang, Y. Song, H. Ji, Q. Ouyang, Y. Wang and L. Jiang, *J. Am. Chem. Soc.*, 2008, **130**, 8345.

13 S. Umehara, N. Pourmand, C. D. Webb, R. W. Davis, K. Yasuda and M. Karhanek, *Nano Lett.*, 2010, **6**, 2486.

14 Y. Rojanasakul and J. R. Robinson, *Int. J. Pharm.*, 1989, **55**, 237.

15 S. B. Lee and C. R. Martin, *Anal. Chem.*, 2001, **73**, 768.

16 (*a*) M. Ali, B. Yameen, J. Cervera, P. Ramírez, R. Neumann, W. Ensinger, W. Knoll and O. Azzaroni, *J. Am. Chem. Soc.*, 2010, **132**, 8338; (*b*) B. Yameen, M. Ali, R. Neumann, W. Ensinger, W. Knoll and O. Azzaroni, *Nano Lett.*, 2009, **9**, 2788; (*c*) B. Yameen, M. Ali, R. Neumann, W. Ensinger, W. Knoll and O. Azzaroni, *J. Am. Chem. Soc.*, 2009, **131**, 2070.

17 (*a*) Y. Maekawa, Y. Suzuki, K. Maeyama, N. Yonezawa and M. Yoshida, *Langmuir*, 2006, **22**, 2832; (*b*) J. Li, Y. Maekawa, T. Yamaki and M. Yoshida, *Macromol. Chem. Phys.*, 2002, **203**, 2470.

18 C. A. Pasternak, G. M. Alder, D. T. Edmonds, C. W. Pitt, C. Terrace, P. Road, S. Petersburg and S. Petersburg, *Radiat. Meas.*, 1995, **25**, 675.

19 (*a*) J. Marchand-Brynaert, M. Deldime, I. Dupont, J.-L. Dewez and Y.-J. Schneider, *J. Colloid Interface Sci.*, 1995, **173**, 236; (*b*) A. Papra, H. G. Hicke and D. Paul, *J. Appl. Polym. Sci.*, 1999, **74**, 1669; (*c*) A. Mara, Z. Siwy, C. Trautmann, J. Wan and F. Kamme, *Nano Lett.*, 2004, **4**, 497; (*d*) M. Ali, B. Schiedt, K. Healy, R. Neumann and W. Ensinger, *Nanotechnology*, 2008, **19**, 085713.

20 Y. S. Lee, *Self-Assembly and Nanotechnology: A Force Balance Approach*, Wiley-Interscience, New York, 2008, pp. 125–145.

21 M. Ramanathan, L. K. Shrestha, T. Mori, Q. Ji, J. P. Hill and K. Ariga, *Phys. Chem. Chem. Phys.*, 2013, **15**, 10580.

22 (*a*) J. Du, Y. Tang, A. L. Lewis and S. P. Armes, *J. Am. Chem. Soc.*, 2005, **127**, 17982.

23 J.-L. Popot, T. Althoff, D. Bagnard, J.-L. Banères, P. Bazzacco, E. Billon-Denis, L. J. Catoire, P. Champeil, D. Charvolin, M. J. Cocco, G. Crémel, T. Dahmane, L. M. de la Maza, C. Ebel, F. Gabel, F. Giusti, Y. Gohon, E. Goormaghtigh, E. Guittet, J. H. Kleinschmidt, W. Kühlbrandt, C. Le Bon, K. L. Martinez, M. Picard, B. Pucci, J. N. Sachs, C. Tribet, C. van Heijenoort, F. Wien, F. Zito and M. Zoonens, *Annu. Rev. Biophys.*, 2011, **40**, 379.

24 X. Hou, H. Dong, D. Zhu and L. Jiang, *Small*, 2010, **6**, 361.

25 (*a*) B. Schiedt, K. Healy, A. P. Morrison, R. Neumann and Z. Siwy, *Nucl. Instrum. Methods Phys. Res., Sect. B*, 2005, **236**, 109; (*b*) J. H. Wang and C. R. Martin, *Nanomedicine*, 2008,

3, 13–20; (*c*) E. B. Kalman, O. Sudre, I. Vlassiouk and Z. S. Siwy, *Anal. Bioanal. Chem.*, 2009, **394**, 413–419; (*d*) B. Yameen, M. Ali, R. Neumann, W. Ensinger, W. Knoll and O. Azzaroni, *Small*, 2009, **5**, 1287–1291.

26 S. J. Kim, Y.-C. Wang, J. H. Lee, H. Jang and J. Han, *Phys. Rev. Lett.*, 2007, **99**, 044501.

27 V. M. Barragán and C. Ruíz-Bauzá, *J. Colloid Interface Sci.*, 1998, **205**, 365–373.

28 J. Drelich, J. L. Wilbur, J. D. Miller and G. M. Whitesides, *Langmuir*, 1996, **12**, 1913–1922.

29 M. Ali, S. Nasir, P. Ramirez, J. Cervera, S. Mafe and W. Ensinger, *ACS Nano*, 2012, **6**, 9247.

30 B. Yameen, M. Ali, R. Neumann, W. Ensinger, W. Knoll and O. Azzaroni, *J. Am. Chem. Soc.*, 2009, **131**, 2071.

31 I. Enculescu, Z. Siwy, D. Dobrev, C. Trautmann, M. E. Toimil-Molares, R. Neumann, K. Hjort, L. Westerberg and R. Spohr, *Appl. Phys. A*, 2003, **77**, 751–755.

32 C. C. Harrell, P. Kohli, Z. Siwy and C. R. Martin, *J. Am. Chem. Soc.*, 2004, **126**, 15646–15647.

33 C. R. Martin, *Science*, 1994, **266**, 1961–1966.